Lab on a Chip

RSC Publishing

HIGHLIGHT

View Article Online
View Journal | View Issue

Research highlights

Cite this: *Lab Chip*, 2013, **13**, 3778
Received 30th July 2013,
Accepted 30th July 2013

DOI: 10.1039/c3lc90085a

www.rsc.org/loc

Šeila Selimović,[ab] Mehmet R. Dokmeci[ab] and Ali Khademhosseini*[abcd]

Nanocrystals on-demand

When it comes to physical processes like crystal nucleation and growth, microfluidics has offered multiple reliable techniques, especially with respect to organic materials (*e.g.* protein crystallization). An attractive trait of this technology is its ability to control the kinetic path of the solute, *e.g.* by progressively concentrating the protein on-chip, or changing the level of supersaturation.[1,2] Similarly, the generation of droplets inside microfluidic channels has introduced a new platform to perform biological and chemical assays. Leveraging microdroplet technology, numerous chemical processes can be conducted under well controlled conditions for large scale industrial applications.

Noble-metal nanocrystals are known for their catalytic properties. Palladium (Pd) crystals, for example, are used to accelerate redox reactions or hydrogenation, but only high-quality, pure crystals with a narrow size distribution are desired.[3] Previous efforts to employ microfluidics for generation of such crystals have utilized diffusion-based mixing. The resulting differences in residence or mixing times, *e.g.* inside continuous flow microfluidic chambers, have resulted in a wide range of crystal size dimensions. Now, Xia[4] and researchers have employed a ''quick fix'' that vastly narrows the size distribution and the number of crystal morphologies.

In their approach, Kim *et al.*[4] employed a standard water-in-oil emulsion setup using silica capillaries (Fig. 1a). Three reagents R1, R2 and R3 (a palladium-containing precursor, a stabilizer, and a reducing agent) were introduced into the capillaries using syringe pumps while an additional capillary carried silicone oil as the sheath fluid. The four fluids were then merged together at an intersection where aqueous droplets of equal size were formed at uniform intervals.

To induce rapid mixing of the fluids, the architecture of the mixing zone was modified (Fig. 1b). Specifically, the PTFE tubing was pinched and partially flattened every 4 mm along the full mixing length (50 mm). Each of these nozzles caused the deformation of droplets and enabled the onset of chaotic advection. Compared to flow through a straight piece of tubing, where mixing would be solely governed by diffusion, here mixing was accelerated and more controlled. An incubation zone (~3.5 m long piece of tubing) followed after the mixing region, in which the nanocrystals were allowed to grow to the desired size. Finally, the tubing was fed into a glass vial filled with distilled water. The droplets containing nanocrystals entered this aqueous solution where the silicone oil was collected from the top, enabling efficient isolation of the Pd nanocrystals.

In addition to the control over size distribution, this microfluidic setup also allowed the researchers to adjust the crystal shape, size, and morphology simply by altering the relative concentrations of the three reagents by adjusting their individual flow rates. Thus, the presented microfluidic platform offers multiple advantages for large-scale industrial

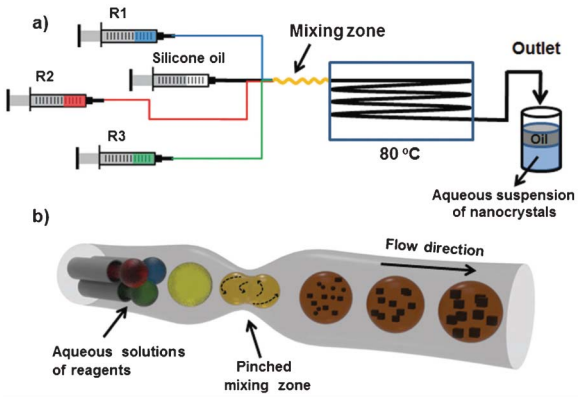

Fig. 1 Schematic of the microfluidic setup with 3 crystallization components and silicone oil as the sheath fluid (a), all of which are combined in microdroplets until nanocrystals can be harvested. The flow junction, where the droplets are generated, and the pinched mixing zone are magnified in the schematic in (b). Image reprinted with permission from Kim *et al.*[4]

[a]*Center for Biomedical Engineering, Department of Medicine, Brigham and Women's Hospital, Harvard Medical School, Cambridge, Massachusetts 02139, USA. E-mail: alik@rics.bwh.harvard.edu*
[b]*Harvard-MIT Division of Health Sciences and Technology, Massachusetts Institute of Technology, Cambridge, Massachusetts 02139, USA*
[c]*Wyss Institute for Biologically Inspired Engineering, Harvard University, Boston, Massachusetts 02115, USA*
[d]*World Premier International – Advanced Institute for Materials Research (WPI-AIMR), Tohoku University, Sendai 980-8577, Japan*

applications. In particular, the use of silica capillaries and PTFE tubing reduced the need for microfabrication. In addition, the seemingly trivial alteration of a standard tubing introduced chaotic advection, thereby greatly minimizing the mixing time and reducing the crystal size distribution. Furthermore, the morphology and the overall crystal size could be modified simply by reprogramming the syringe pumps. This creative setup has the potential to transform a standard platform into a more efficient system for large-scale production.

Microfluidic Raman scattering sensors

The detection and quantification of chemical and biological agents is important for various applications such as disease diagnostics, food and drug testing and environmental monitoring. In all these fields it is vital to detect and identify trace components, with high accuracy, precision and ideally in real-time.

Several techniques that can detect and distinguish similar molecules are based on light scattering, such as Raman spectroscopy.[5] In this phenomenon, a small subset of photons (*e.g.* from a laser source) incident on a molecule are scattered inelastically, that is, the frequency of the scattered photons is different from that of the incident photons. The difference in frequency is highly specific to the type of molecule, enabling the identification of sample constituents. The Raman scattering signal can be greatly enhanced by placing the sample on a roughened metal surface. It is predicted that in this surface-enhanced Raman scattering (SERS) platform the electric field of the substrate is enhanced when the frequencies of the incident photons and the substrate-bound excitations (plasmons) are in resonance. This method can be applied for the detection of trace quantities of a sample, and even single molecules.[6] To perform SERS-based detection of biomolecules, a necessary step is to merge this technology with microfluidics.

Mao *et al.*[7] recently developed a SERS-enabled microfluidic chip by combining poly(dimethylsiloxane) (PDMS) and photopatterned metallic nanopillars. The fluidic component was simple, consisting of a single straight channel (~few tens of microns wide) with inlet/outlet ports (Fig. 2a–d). The SERS active region was created from a gold-coated forest of nanopillars fabricated using oxygen-plasma stripping of photoresist. Here, a substrate was patterned with photoresist and subsequently stripped with an oxygen plasma. Under certain plasma processing conditions the resulting photoresist ash was polymerized to form nanoscale residues in the shape of dots and fibers. The researchers also managed to generate larger-scale ''nanoforests''. Here, they began with the nanoscale residues as the master mold, coated it with a SiO_2 layer, and then produced large nanopillar arrays using reactive ion etching. On average, the nanopillars were 1.4 μm tall and ~300 nm in diameter, with a relatively high density of 8 per μm^2 (Fig. 2e and f). Finally, the nanoforests were coated with a thin layer of gold or silver. This additional layer helped close some of the gaps between the nanopillars, giving rise to ''hot-spots'' – areas on the substrate particularly conducive to SERS signals.

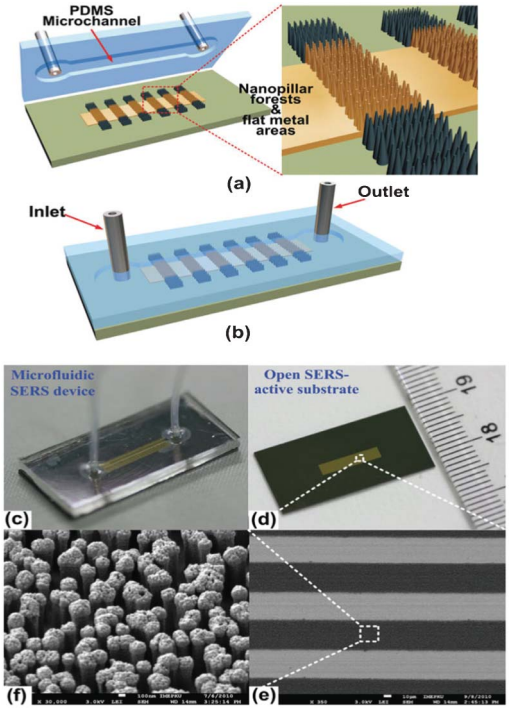

Fig. 2 Schematics of the microfluidic SERS chip (a), (b); photographs of the chip (c) and the SERS-active surface (d); SEM images of the photopatterned SERS active surface (e), (f). Figure adapted and reprinted with permission from Mao *et al.*[7]

The SERS-chip was evaluated by using different concentrations of rhodamine ranging nM to mM. The dye solution was flowed through the chip and allowed to evaporate, yielding a uniform layer of rhodamine on the nanopillars. In another set of tests, the same sample volume was dispensed onto the nanoforest without the PDMS cover. After evaporation, the rhodamine coating was found to be much less uniform, due to the convective processes inside the rhodamine droplet. As a result, the measurements obtained from the microfluidic chip with a cover had higher repeatability across the chip than the open version of the chip (all measurements were conducted using a confocal Raman microscope with a He–Ne laser). Nonetheless, the PDMS cover likely absorbed some of the incident and scattered light, reducing the chip sensitivity by a factor of 4.

Thus, a key advantage of the microfluidic SERS comes from uniform deposition of the sample molecules on the substrate and decreased experimental error. The signal could potentially be boosted by using a thinner layer of PDMS or a different material as the cover for the chip. Alternatively, it may be possible to install an array of microscale detectors inside the microfluidic channel, thereby eliminating the need for a highly transparent cover. Finally, it should be noted that the use of exceedingly small reagent volumes also reduced the

detection time from hours to minutes. This makes the microfluidic SERS sensor particularly suited for the detection of environmentally sensitive trace molecules like proteins.

Optofluidic monitoring of live cells

Cell secretion is an important indicator of cell activity, and as a consequence, of an individual's health. This is particularly true in diagnostics of immune responses, *e.g.* inflammation or cancer occurrences. To better understand the underlying processes in these immune responses, it is necessary to monitor cell secretion in real-time and with high sensitivity. Laboratory methods like immunoassays only offer snapshots of cell secretion activity, while time-lapse microscopy based on detection of fluorescent species requires cell labeling and/or genetic modification of cells. Neither approach is ideal, as the cells should remain unaffected by the experimental procedure, and real-time observation of the cellular behavior is required to understand the underlying dynamic processes.

An emerging technique that could address both requirements involves Fano resonance.[8] This is a type of light scattering that relies on the interference between the background signal and the resonant scattering between the incident light and the light that scatters off a molecular sample. The sample can be an inorganic molecule or a biological one, such as a protein bound to a substrate. First, incident light with a particular wavelength is chosen, then the intensity of the light scattering off of or being transmitted through a sample can be detected with a microscope and further quantified by a spectrometer, allowing for real-time observation. The team led by Cheng and Wei has recently utilized Fano resonance to detect the presence of cell secretory proteins inside a well-controlled microscale environment within a microfluidic chip.

In this work, Wu *et al.*[9] loaded a suspension of leukemia cells (type THP1) into a simple microfluidic chip and trapped them individually inside an array of U-shaped trapping structures (Fig. 3b–d). Next, lipopolysaccharide (LPS) was added to the microfluidic chip. LPS is known to elicit the secretion of a metalloproteinase (MMP), which plays a factor in a host of diseases such as arthritis and tumor metastasis. A key novelty of the chip was the top cover layer which, instead of PDMS, was made from a polycarbonate film patterned with a gold nanoslit array on top of which a monolayer of antibodies was patterned to allow for MMP binding (Fig. 3a).

Shortly after the cells were exposed to LPS, they started to secrete MMP, which almost immediately bound to the antibodies. Specifically, the distance between a cell and the antibody-layer on the polycarbonate surface was only a few microns, which reduced the diffusion time of the secreted proteins. Therefore, the amount of secreted proteins was assumed to be linearly proportional to the amount of bound proteins on the chip, with the lowest detectable concentrations in the order of ng mL^{-1}. The bound proteins affected the intensity of the transmitted light at particular wavelengths, so

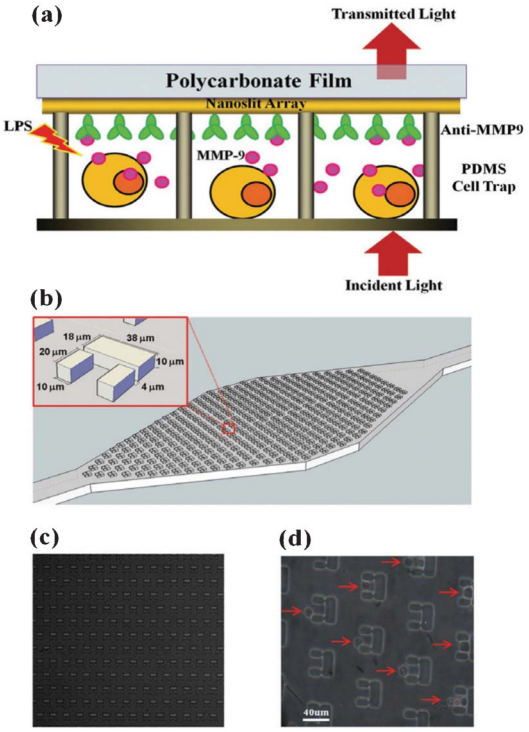

Fig. 3 Schematic of the experimental setup. (a): cells are individually captured in traps, where the secreted proteins bind to the antibodies. The intensity of the transmitted light is proportional to the amount of bound proteins. The device is sketched in (b). Optical images of the trap array (c) and captured cells (d). Figure reprinted with permission from Wu *et al.*[9]

that the spectroscopic light intensity measurements were directly correlated to the amount of attached proteins. Importantly, the experiments revealed that the cells secreted a finite amount of MMP regardless of the LPS concentration, indicating that there could be an internal MMP reservoir in the cells. Then, the supplied LPS began to trigger an increase in MMP secretion until a second plateau was reached. Thus, this real-time observation allowed a new inspection mechanism for the secretory dynamics of the leukemia cell type. Incidentally, the same results were obtained from two as well as from several hundred cells, indicating that the MMP secretion is a highly stable process that does not vary much from cell to cell.

Most importantly, the presented study did not require cell tagging or genetic modulation of the cells, thereby eliminating potential secondary effects or affecting the MMP production. As shown, it also allowed an opportunity for real-time monitoring of the cell secretory behaviour, which has not been possible by the use of standard protein detection methods. Thus, although Fano resonance is not a widely used technique in biology and bioengineering laboratories, this work could serve to convince others in the field to explore this and other related light scattering phenomena, such as Raman scattering, in conjunction with microfluidics to study real-time dynamics of cell secretion.

References

1 Š. Selimović, F. Gobeaux and S. Fraden, *Lab Chip*, 2010, **10**, 1696–1699.
2 C. L. Hansen, E. Skordalakes, J. M. Berger and S. R. Quake, *Proc. Natl. Acad. Sci. U. S. A.*, 2002, **99**, 16531–16536.
3 T. Teranishi and M. Miyake, *Chem. Mater.*, 1998, **10**, 594–600.
4 Y. H. Kim, L. Zhang, T. Yu, M. Jin, D. Qin and Y. Xia, *Small*, 2013, DOI: 10.1002/smll.201203132.
5 P. Etchegoin, R. C. Maher, L. F. Cohen, H. Hartigan, R. J. C. Brown, M. J. T. Milton and J. C. Gallop, *Chem. Phys. Lett.*, 2003, **375**, 84–90.
6 K. Kneipp, Y. Wang, H. Kneipp, L. T. Perelman, I. Itzkan, R. R. Dasari and M. S. Feld, *Phys. Rev. Lett.*, 1997, **78**, 1667–1670.
7 H. Mao, W. Wu, D. She, G. Sun, P. Lv and J. Xu, *Small*, 2013, DOI: 10.1002/smll.201300036.
8 B. Luk'yanchuk, N. I. Zheludev, S. A. Maier, N. J. Halas, P. Nordlander, H. Giessen and C. T. Chong, *Nat. Mater.*, 2010, **9**, 707–715.
9 S.-H. Wu, K.-L. Lee, A. Chiou, X. Cheng and P.-K. Wei, *Small*, 2013, DOI: 10.1002/smll.201203125.